MASTER THESIS

Spectral Analysis of Directed Complex Networks

Tetsuro Murai

Department of Physics,
Graduate School of Science and Engineering,
Aoyama Gakuin University

Supervisors: Naomichi Hatano and Kenn Kubo

2002

MASTER THESIS
Spectral analysis of directed complex networks

Tetsuro Murai (35101017)
Supervisors: Naomichi Hatano and Kenn Kubo

March 20, 2003

Department of Physics,
Graduate College of Science and Engineering,
Aoyama Gakuin University
Chitosedai 6-16-1, Setagaya, Tokyo 157-8572, Japan

Abstract

Various natural and social systems develop complex networks and many of them have directed links. In recent years, many studies analyze the topology and dynamics of complex networks. Most of them, however, focus on the property of undirected networks; directed networks are treated as a naive extension of undirected networks. Our main question is the following: what could possibly happen if a network has directed edges? Do they really act like the undirected ones?

In the present thesis, we discuss properties of networks generated by the directed edges. We particularly focus on a typical direction of links, which we call the *flow* in a network. We expect that some of real networks have flows. We show that we can detect a flow in a directed network by analyzing the complex spectrum of the adjacency matrix of the network. We also report further results obtained from the spectral analysis.

Contents

1 Introduction

Many complex systems in nature as well as in our society have complex network structure in them. The network structure is an important feature of the complex systems and worth an extensive study. We can treat the network structure of many complex systems with a common mathematical tool, namely the “graph theory,” by defining the nodes (vertices) and the links (edges) connecting the nodes. For example, the World Wide Web is well described as a graph by taking the web pages as nodes and the hyperlinks connecting the pages as edges. The Internet is also a complex network with computers and routers as nodes and the physical links between them as edges. The network of scientific collaboration is an example of the network in social systems. In this network the nodes are the scientists and two nodes are connected by an edge if the two scientists have written an article together.

Traditionally, the structural property of complex systems has been modelled as random graphs. Until recently, the uncorrelated random graph model, which was first studied by Erdős and Rényi [1] in the 1950s, has been the main tool of analyzing the complex systems. In the Erdős-Rényi model, we start with N nodes and connect every pair of nodes with a probability p. Then we obtain a graph with approximately $pN(N-1)/2$ edges randomly distributed; The graph seems like a complex network for large N. The Erdős-Rényi model has itself many interesting properties and has been studied much in the mathematical literatures.

It recently turns out, however, that many of the actual networks show common statistical properties which are significantly different from the uncorrelated random-graph model. Motivated by the fact that the real systems show common correlated properties, many studies have tried to clarify the structure of networks in the real world. These efforts have resulted in characterization of the real networks from the viewpoint of the following three concepts: *small world, clustering* and *degree distribution.*

In the next section, we discuss the three main concepts of real networks and introduce the models which we use for calculation. In section 3, we analyze the spectra of undirected network models. Finally in section 4, we show the spectral analysis of directed network models. We discuss the relation between the network flow and the structure of the spectrum and some further results we obtained from the spectra.

2 Characterization and modeling of real networks

2.1 Topology of real networks

In this section, we briefly discuss the three main concepts of the real networks.

Small world: The concept of the small world is based on the fact that in most networks there is a relatively short path between any two nodes despite their often large size [2, 3]. The distance between two nodes is defined as the number of edges along the shortest path connecting them. The *average path length* ℓ of a network is the average of the distance between all the possible pairs of nodes in the network. Recent studies have shown that a relatively small ℓ is a basic character of the real networks. For example, Broder *et al.* [4] analyzed 2×10^8 web pages on the WWW and found that the average path length ℓ is about 16.

Note that the small-world behavior does not necessarily indicate the correlated property of the real networks. In fact the Erdős-Rényi random-graph model also displays the small-world character. In a random graph with N nodes and $\langle k \rangle$ edges on average for each node, the number of steps d which satisfies

$$\langle k \rangle^d \approx N \tag{1}$$

is enough to connect any two nodes in the network. Thus the typical distance between any two nodes in a random graph scales as the logarithm of the number of nodes. As explained below, many real networks have the characters of the small world *and* high clustering.

Clustering: Clusters of nodes appear in many systems: for example, research groups in the network of scientific collaboration and circles of friends in the network of human relationship. To quantify the extent of the cluster, the *clustering coefficient* is often used [2, 3]. The clustering coefficient of a node i with k_i edges is defined as follows: first, we consider a subgraph consisting of the k_i neighbors of the node i. Note that the subgraph excludes the node i. If all the k_i nodes are connected to each other, there are $k_i(k_i - 1)/2$ edges in the subgraph. The ratio between the number E_i of the edges that actually exists in the subgraph and the maximum possible number $k_i(k_i - 1)/2$ gives the clustering coefficient of the node i:

$$C_i = \frac{2E_i}{k_i(k_i - 1)}. \tag{2}$$

In other words, the clustering coefficient of the node i is the probability that two of the neighbors of the node i are also connected. The clustering coefficient C of the whole network is the average of C_i over all i.

In the random graph the probability that two of the neighbors of a node are connected is equal to the probability that two randomly chosen nodes are connected. Thus the clustering coefficient of a random graph is

$$C_{\text{rand}} = p = \frac{\langle k \rangle}{N}, \tag{3}$$

which becomes very small for large N. The clustering coefficient of most real networks are known to be much larger than that of a random network with the same N and $\langle k \rangle$. This directly indicates the correlated nature of real networks.

In general, we cannot estimate the behavior of the average path length from Eq. (1) because of the clustering. The number of nodes we can visit by t steps is approximately $(1 - C)^{t-1}\langle k \rangle^t$. Thus a network with a large clustering coefficient seems to have a large path length. However, many of the real networks show both the small-world character *and* the clustering property, that is, a small path length and a large clustering coefficient at the same time. In practice, the name "small-world network" is often used for networks with these two properties.

Degree distribution: The degree distribution $P(k)$ of a network is a distribution function which gives the probability that a randomly chosen node has exactly k edges. In the random graph with large N, the degree distribution becomes a Poisson distribution. In many real networks, however, the degree distribution has a power-law form:

$$P(k) \sim k^{-\gamma}. \tag{4}$$

Such networks are called *scale-free networks* [5]. All the real networks we introduced as examples are known as scale-free networks [4, 6, 7, 8, 9, 10, 11].

2.2 Model of the small-world network

Real networks have the small-world character like random graphs, but they also have unusually large clustering coefficient. The first successful attempt to generate graphs with a large clustering coefficient and a small path length was made by Watts and Strogatz [2]. They proposed a one-parameter model that interpolates between an ordered finite dimensional lattice and a random graph. The generating algorithm of the Watts-Strogatz model is as follows (Fig. 1): We start with a ring lattice with N nodes. Every node is connected to its first k neighbors ($k/2$ on each side). Then we randomly rewire each edge of the lattice with probability p. By varying p we can closely monitor the transition between order ($p = 0$) and randomness ($p = 1$).

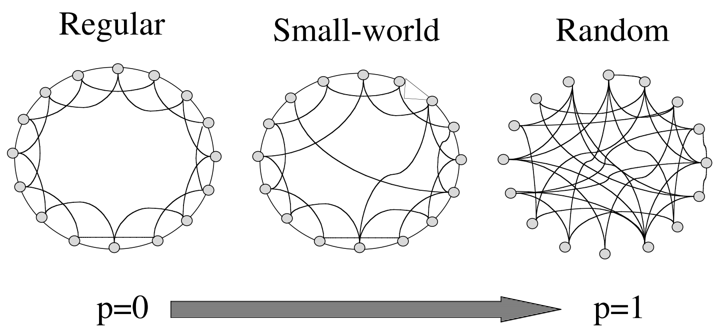

Figure 1: An example of the Watts-Strogatz model with $\langle k \rangle = 4$. The initial state is the regular ring graph; We add randomness with probability p.

To understand the coexistence of a small path length and high clustering, we study the behavior of the clustering coefficient $C(p)$ and the average path length $\ell(p)$ as the functions of the rewiring probability p. As shown in Fig. 2, the regular lattice ($p = 0$) yields a high clustering coefficient and a large path length, while the random graph ($p = 1$) yields a low clustering coefficient and a small path length. However, a large C and a small ℓ coexist in the broad region of intermediate value of p, which characterizes the small-world network. The reason of the appearance of the small-world network is that $\ell(p)$ drops rapidly at a small value of p, while $C(p)$ stays almost unchanged.

The Watts-Strogatz model indicates that the small-world network exists in the region between order and randomness, and so is the real networks.

2.3 Directed networks

Many complex networks that appear in natural and social sciences have directed links. Consider the World Wide Web, for example; if the Web page A has a hyperlink to the Web page B, it does not necessarily mean that the Web page B has a hyperlink to the Web page A. The predator-prey relationships in food webs is another example of directed links. Despite the existence of directions in many real networks, most studies of complex networks have focused mainly on undirected networks.

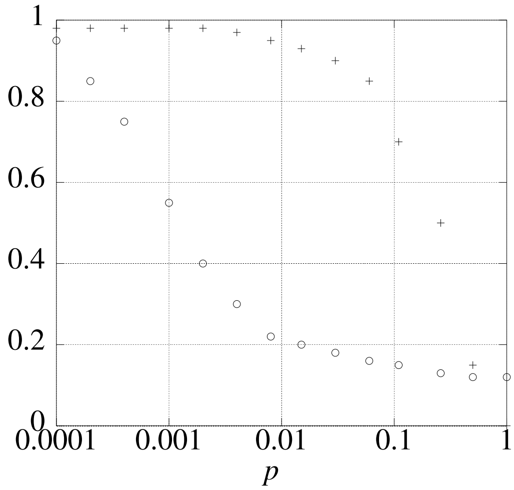

Figure 2: The p dependence of ℓ and C of the Watts-Strogatz model. The circles indicate $\ell(p)/\ell(0)$ and the crosses $C(p)/C(0)$. In an intermediate value of p, the network shows a large C and a small ℓ at the same time, which is a typical character of real networks.

In the present thesis, we investigate the effects of directed links in small-world networks which interpolate between a regular lattice network and a random network. We particularly focus on a typical direction of links, which we call a *flow* in a network (Fig. 3). It is possible that small-world networks have flows since small-world networks are not completely random. In a limiting case, all links have the same direction in a directed regular lattice, and hence there is a flow (See the right graph of Fig. 3).

We expect that some of the real networks actually have flows. For example, consider the hierarchical structure of a food web known as the pyramid of food chain. The direction of the predator-prey relationship is from the top of the pyramid to the bottom of it. Another example is the citation network. In the citation network, nodes stand for published articles and a directed edge represents reference to a previously published article. Since reference is made only for an article previously published, the typical direction of links are from future to past. If we follow the references of the latest article in a field, we will soon get most of the important articles in that field. But we never find the latest work if we start from an older paper. In other words, the knowledge of science *flows* from past to future through the citation networks.

How can we detect the flow in a network? Since graphs have no spatial measure, it is difficult to find a flow in a network with randomness (Fig. 4). We show that complex eigenvalues of the adjacency matrix of directed net-

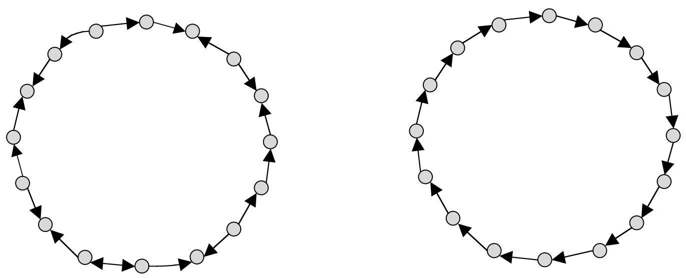

Figure 3: If undirected, these two networks would be equal. With directions, can we treat them equally? The left network does not have a *flow*, but the right one does.

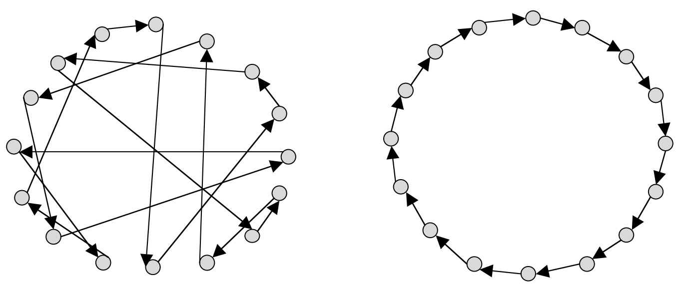

Figure 4: As a graph, these two networks are equivalent. The left network however, seems to have no typical direction. How do we know whether there is a flow in the left network?.

works contain a lot of useful information, especially information on the *flow* in the network.

2.4 Directed Watts-Strogatz model

In the present thesis, we introduce an extension of the Watts-Strogatz model to make directed networks which interpolates between the regular network and the random network. The directed Watts-Strogatz model is given as follows: We first prepare a regular lattice as in the undirected model. We then assign the direction to each edge in the following way: each edge may be directed clockwise with probability p_1, counterclockwise with probability p_2, and bidirectional with probability $1 - p_1 - p_2$. Thus obtained directed graph is the initial state. Then we randomly rewire each directed edge of the lattice with probability p under the condition that self-connections and multiple edges are excluded. To examine the effect of *flow* in the network, we hereafter use two types of the initial state and refer to them as the models A and B. Their initial states are chosen as

Model A: $p_1 = 0.5,\ p_2 = 0.5,$

Model B: $p_1 = 1,\ p_2 = 0,$

respectively (Fig. 5).

For any directed networks, the average degree of the incoming edges $\langle k_{\rm in}\rangle$ and the outgoing edges $\langle k_{\rm out}\rangle$ are always equal. Thus we write the average degree of directed networks as

$$\langle k\rangle \equiv \langle k_{\rm in}\rangle = \langle k_{\rm out}\rangle. \tag{5}$$

In Fig. 5, we specifically chose the case $\langle k\rangle = 2$.

3 Spectra of undirected networks

The spectra of undirected small-world networks were first analyzed by Farkas *et al.* [12]. We review discussions on the spectra of undirected networks in this section.

3.1 Definitions

The graph we consider in the present thesis is a set of points (nodes or vertices) connected by lines (edges or links). The edges may be directed or undirected. We refer to the graphs consisting only of undirected edges as *undirected graphs* and to the graphs which include directed edges as *directed*

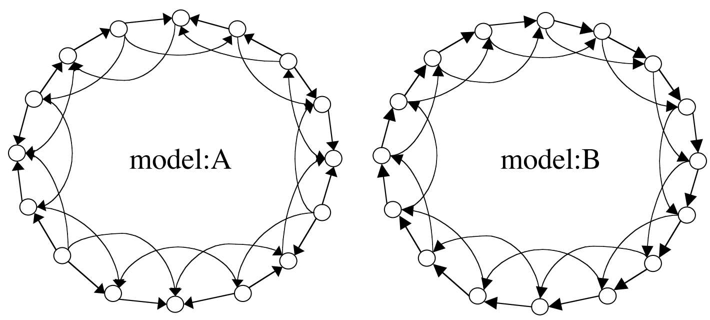

Figure 5: The initial states of the models A and B have the same topology but different directions of edges. These figures are an example of the regular lattice with $\langle k \rangle = 2$.

graphs. We consider only graphs without any unit loop which connect a node to itself and any multiple edges between a pair of nodes.

Any graph can be represented by its adjacency matrix A. The definition of the adjacency matrix of an undirected graph is as follows:

$$A_{ij} = A_{ji} = \begin{cases} 1, & \text{if node } i \text{ and node } j \text{ are connected.} \\ 0, & \text{if node } i \text{ and node } j \text{ are not connected.} \end{cases}$$

We analyze graphs using the spectrum of the graph, or the set of the eigenvalues of the graph's adjacency matrix. The meaning of the eigenvalues and the eigenvectors of a graph can be illustrated by the following example. Suppose that each component of a vector $\vec{v}$ is a quantity v_i on each node i. Operating A to $\vec{v}$ means to rewrite the quantities on each node by the following rule: the quantity on node i becomes the sum of the quantities on the nodes which have an edge toward node i. If the resulting vector is a multiple of $\vec{v}$, then $\vec{v}$ is an eigenvector and the multiplier is the corresponding eigenvalue of the graph.

The spectral density of a graph is the density of the eigenvalues of its adjacency matrix. For a finite system, this can be written as the sum of delta functions

$$\rho(\lambda) \equiv \frac{1}{N}\sum_{j=1}^{N}\delta(\lambda-\lambda_j), \tag{6}$$

which converges to a continuous function as $N \to \infty$.

The spectral density of a graph can be directly related to the graph's topological features: the kth moment, M_k, of $\rho(\lambda)$ can be written as

$$M_k = \frac{1}{N}\sum_{j=1}^{N}(\lambda_j)^k = \frac{1}{N}\mathrm{Tr}(A^k) = \frac{1}{N}\sum_{i_1,i_2,\cdots i_k} A_{i_1,i_2}A_{i_2,i_3}\cdots A_{i_k,i_1}. \tag{7}$$

From the topological point of view, $L_k = NM_k$ is the number of directed paths (loops) in the graph that return to their starting node after k steps. Note that these paths can contain nodes that were already visited. Since $\langle\lambda\rangle \propto \mathrm{Tr}A = 0$, the variance of $\rho(\lambda)$ represents the number of edges and its skewness represents the number of triangles in the network.

3.2 Numerical results

In this section, we show the results for undirected network models. First, we show the results for the undirected random graphs. Then, we show the results for the undirected Watts-Strogatz model for various values of p and discuss the relation between the network structure and the spectrum.

(1)*Random graph*: The spectrum of a random graph has been studied mathematically in the random graph theory. It is known that in the $N \to \infty$ limit, the rescaled spectral density of the random graph converges to a semi-circular distribution exemplified in Figs. 6 and 7 [12, 13].

A general form of the *semi-circle law* for real symmetric matrices is the following [14]: If A is a real symmetric $N \times N$ uncorrelated random matrix, that is, $\langle A_{ij}\rangle = 0$ and $\langle A_{ij}^2\rangle = \sigma^2$ for every $i \neq j$, and with increasing N each moment of each $|A_{ij}|$ remains finite, then in the $N \to \infty$ limit the spectral density of $A/\sqrt{N}$ converges to the semi-circular distribution:

$$\rho(\lambda) = \begin{cases} (2\pi\sigma^2)^{-1}\sqrt{4\sigma^2-\lambda^2}, & \text{if } |\lambda| < 2\sigma; \\ 0, & \text{otherwise.} \end{cases} \tag{8}$$

This theorem is also known as *Wigner's law*.

Note that many of the semi-circle law's conditions do not hold for the adjacency matrix of the uncorrelated random graph; for example the expectation value of the matrix elements is not zero. Nevertheless, the rescaled spectral density of the uncorrelated random graph converges to the semi-circle law in the $N \to \infty$ limit.

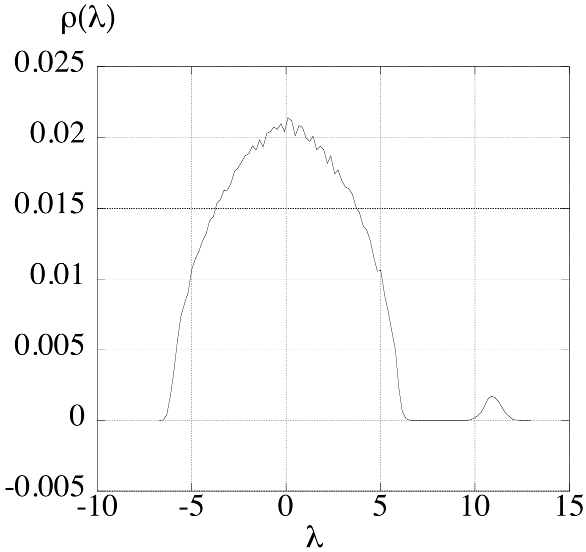

Figure 6: The spectral density of a random graph with $N = 100$ and $\langle k \rangle = 10$. We used one hundred graphs for averaging.

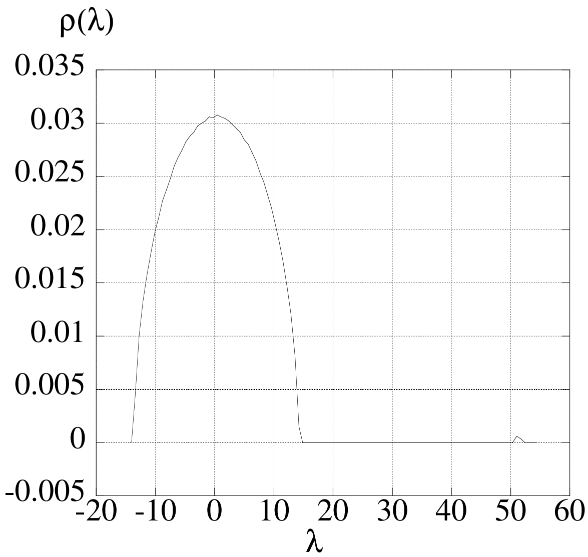

Figure 7: The spectral density of a random graph with $N = 1000$ and $\langle k \rangle = 50$. We used one hundred graphs for averaging.

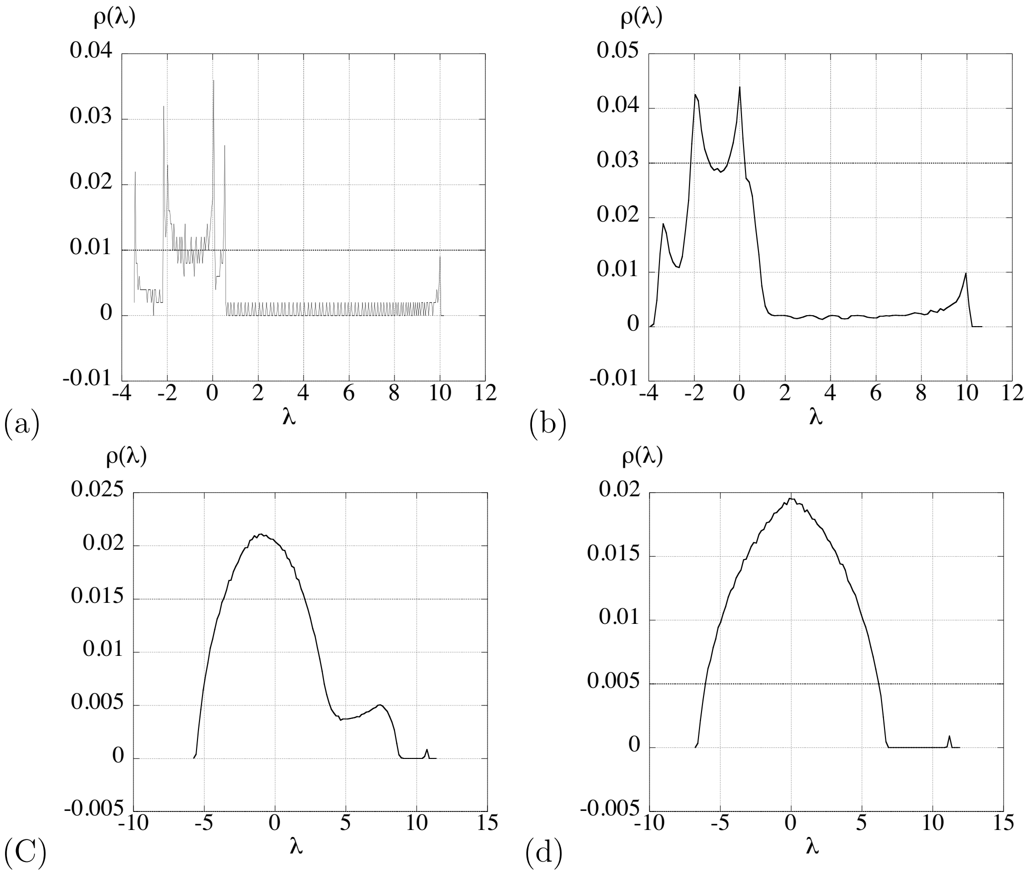

Figure 8: The spectral densities of the undirected Watts-Strogatz model for (a) $p = 0$, (b) $p = 0.01$, (c) $p = 0.3$ and (d) $p = 1$. We used the graphs with $N = 1000$ and $\langle k \rangle = 10$. In (b), (c) and (d) we used one hundred graphs for averaging.

Further results on the behavior of the eigenvalues of the random graph include the following [12, 13]: The principal eigenvalue (the largest eigenvalue, λ_1) grows much faster than the second eigenvalue λ_2. It is known that λ_1 scales as $pN \approx \langle k \rangle$, while λ_2 scales as $\sqrt{N}$. A similar relation holds for the smallest eigenvalue λ_N, which also scales as $\sqrt{N}$. Thus, the "bulk" part of the spectrum scales as $\sigma\sqrt{N}$, whereas the principal eigenvalue grows much faster than that.

(2) *Watts-Strogatz model*: For $p = 0$, the graph of the Watts-Strogatz model is regular and periodical. The spectral density $\rho(\lambda)$ contains numerous singularities because of the highly ordered structure of the initial state (Fig. 8(a)). Note that $\rho(\lambda)$ has a large third moment.

For $p = 0.01$, which is the small-world region of the model, the singularities are smeared, but the distribution still has strong peaks. This indicates that the ordered structure is perturbed, but still dominant in the network (Fig. 8(b)). In $p = 0.3$, there is no sign of sharp peaks characterizing the local ordered structure. However, the third moment is still quite large. This indicates that triangles are still dominant even after the ordered structure is broken (Fig. 8(c)).

Finally, as $p \to 1$, $\rho(\lambda)$ approaches the semi-circle law characterizing random graphs (Fig. 8(d)). While the details of the spectral density changes considerably with p, the third moment of $\rho(\lambda)$ is consistently large, indicating a large number of triangles in the network. Thus we can conclude from the results in Fig. 8 that a large number of triangles is a basic property of the Watts-Strogatz model.

4 Spectra of directed networks

In this section, we show the results of our spectral analysis for the directed random graph and the directed Watts-Strogatz model. We discuss the relations between the network structure and the spectrum from the following points of view: the *flow* in the network, comparison with the spectrum of undirected network and the number of loops in the network.

4.1 Definitions

The adjacency matrix of a *directed* graph is defined as follows:

$$A_{ij} = \begin{cases} 1, & \text{if there is a directed edge from node } i \text{ to node } j. \\ 0, & \text{if there is no edge from node } i \text{ to node } j. \end{cases}$$

Thus, if there is a directed edge from node i to node j and no edge from j to i, $A_{ij} = 1$ and $A_{ji} = 0$. Note that in a directed network, the eigenvalues can be complex since the adjacency matrix is generally asymmetrical.

We remark here some of the important characteristic of the adjacency matrix of a directed graph: The kth moment M_k defined in Eq. (7) is still proportional to the number of loops in the network even for a directed graph. Another important characteristic is that the complex eigenvalues appear in a conjugate pair since A is a real matrix. We can show this from a simple calculation. An eigenvector $\vec{\phi}$ and an eigenvalue λ of a real matrix A can be written in the following form:

$$A\vec{\phi} = \lambda\vec{\phi}. \tag{9}$$

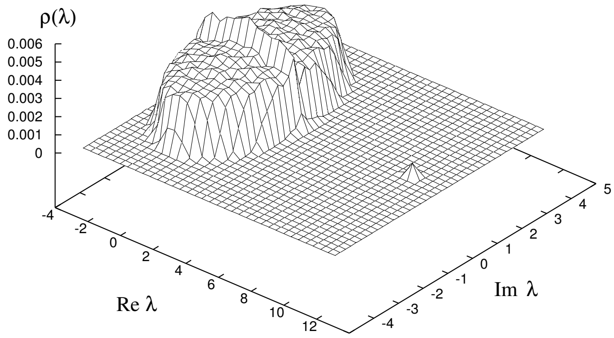

Figure 9: The spectral density of a directed random graph with $N = 1000$ and $\langle k \rangle = 10$. We used one hundred graphs for averaging.

Taking the complex conjugate of Eq. (9), we obtain

$$A\vec{\phi}^* = \lambda^* \vec{\phi}^*. \tag{10}$$

From Eqs. (9) and (10) we see that if λ is a complex eigenvalue of A with the eigenvector $\vec{\phi}$, then λ^* is also an eigenvalue of A corresponding to eigenvector $\vec{\phi}^*$.

4.2 Numerical results

(1) *Directed random graph*: Directed random graphs are made by connecting every pair of nodes with a directed link with a probability p. The spectrum of the directed random graph is a circular distribution in the complex plane (Fig. 9) [14]. The eigenvalue with the largest absolute value λ_1 appears on the real axis. It behaves like the largest eigenvalue of the undirected random graph; that is, it grows much faster than the bulk part of the spectrum.

(2) *Directed Watts-Strogatz model*: We show the results in two limiting cases of the model: The model A starts from a graph with randomly directed edges, whereas the model B starts from a graph with edges ordered clockwise.

(i) $p = 0$: In the initial state, the model A shows a bulk structure (where the eigenvalues are randomly distributed) and a line on the real axis (Fig. 10(a)). In contrast, the model B is well-ordered in the initial state and shows a highly ordered spectrum with a ring structure (Fig. 11(a)). If the edges were undirected, the two initial states would be equivalent. The contrast between these spectra indicates that the spectrum of graphs reflects the effect of directed links sensitively.

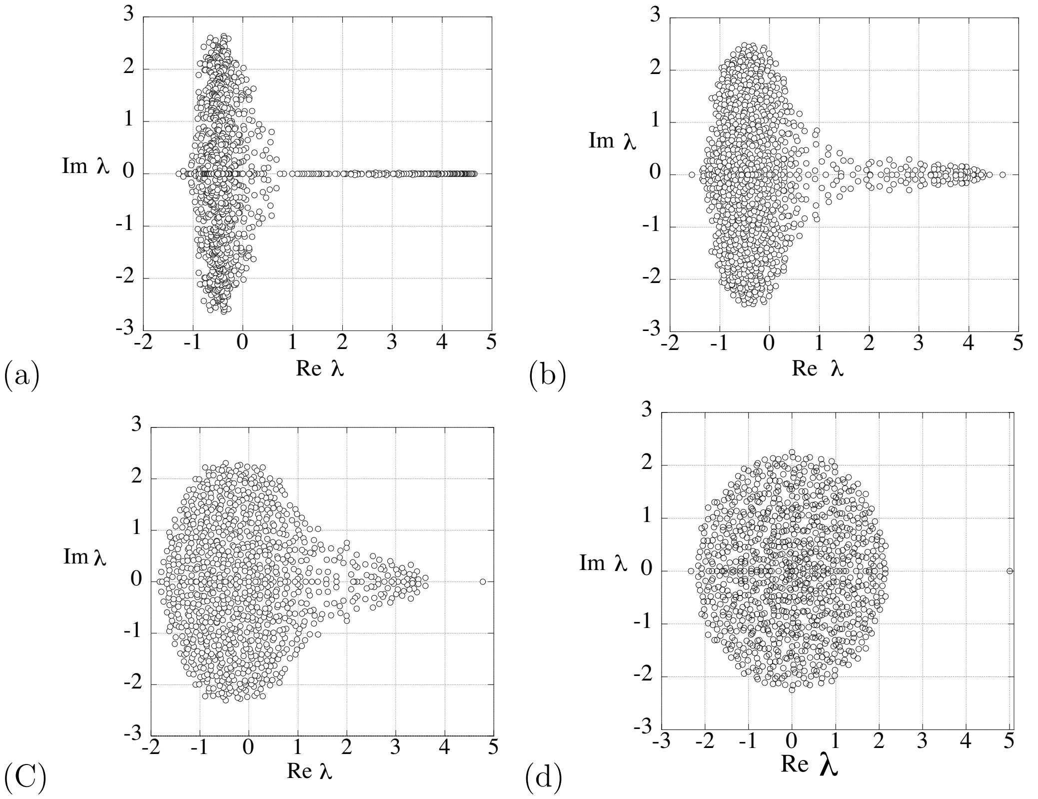

Figure 10: The spectra of the model A for (a) $p = 0$, (b) $p = 0.1$, (c) $p = 0.3$ and (d) $p = 1$. We used graphs with $N = 1000$ and $\langle k \rangle = 5$.
.

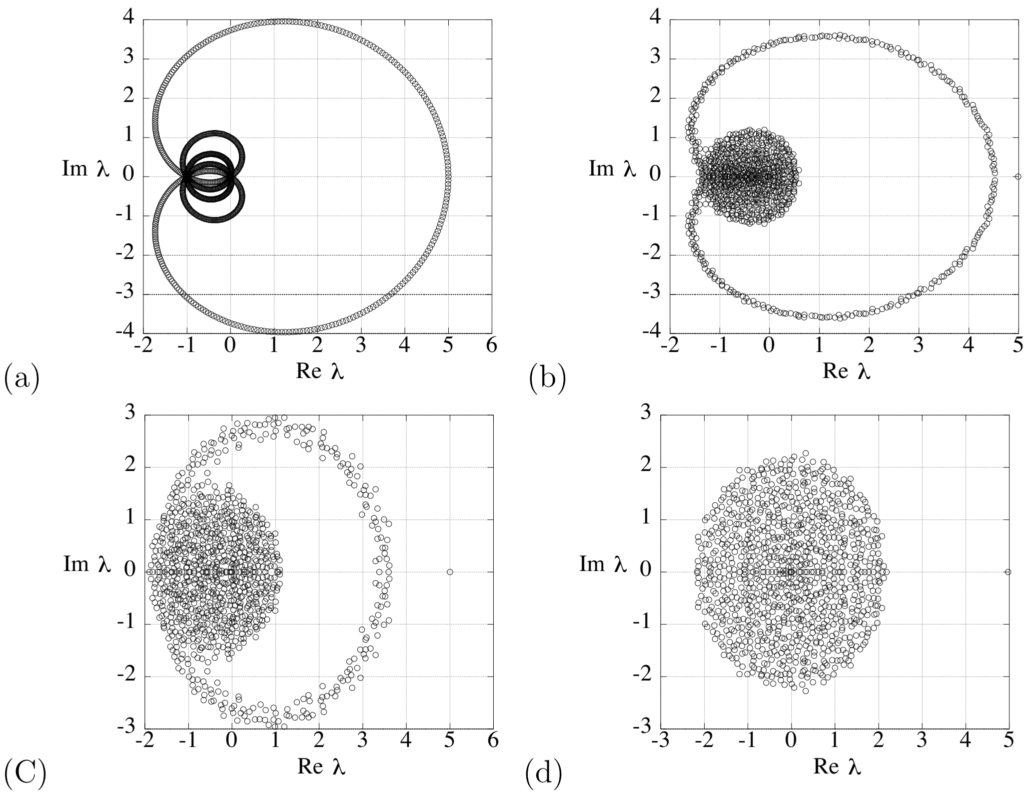

Figure 11: The spectra of the model B for (a) $p = 0$, (b) $p = 0.01$, (c) $p = 0.3$ and (d) $p = 1$. We used graphs with $N = 1000$ and $\langle k \rangle = 5$.

(ii) $1 > p \geq 0.1$: As we increase p, The spectrum of the model A shows a sign of unification of the bulk part and the line part (Fig. 10(b) and (c)). On the other hand, the local ordered structure of the model B vanishes, but the ring structure of its spectrum remains strongly even for large p (Fig. 11(b) and (c)).

(iii) $p = 1$: Finally, the spectra of both models converge to the circular distribution characterizing the random graph (Compare Fig. 10(d) and 11(d) with Fig. 9). In the model A, the bulk part absorbs the line part and the spectrum becomes circular. In the model B, on the other hand, the radius of the ring structure becomes small and the circular distribution is formed. We speculate that the ring structure reflects the *flow* in the network because the most characteristic difference between the two spectra is the ring structure.

4.3 Discussion

(1) *The flow in the network*: The ring structure of a complex spectrum represents the existence of a loop-like *flow* in the network. We can explain this by considering the simplest network with a loop-like flow. Since the initial state of the model B (Fig. 11(a)) has the translational symmetry, we can calculate the eigenvalues analytically by using the Fourier transform. The initial state of the model B is a regular ring graph with N nodes. Each node is connected to its kth neighbors at farthest and the edges are ordered in one direction. The eigenvalues of the graph can be written in the form

$$\lambda_n = \sum_{m=1}^{k} e^{i\frac{2\pi n}{N}m}. \tag{11}$$

In the case of $k = 1$, which is the simple one-dimensional directed chain with a periodic boundary condition, we have

$$\lambda_n = e^{i\frac{2\pi n}{N}}. \tag{12}$$

This forms the unit circle in the complex plane, the simplest ring structure we can consider.

The one-dimensional directed chain is, in other words, a directed loop of N steps. If there is a directed loop of N steps, we obtain N eigenvalues which satisfy

$$\lambda^N = 1. \tag{13}$$

They form a ring in the complex plane. In the case of more complicated loops, that is, regular directed rings with $k \geq 2$, the ring structure is still dominant.

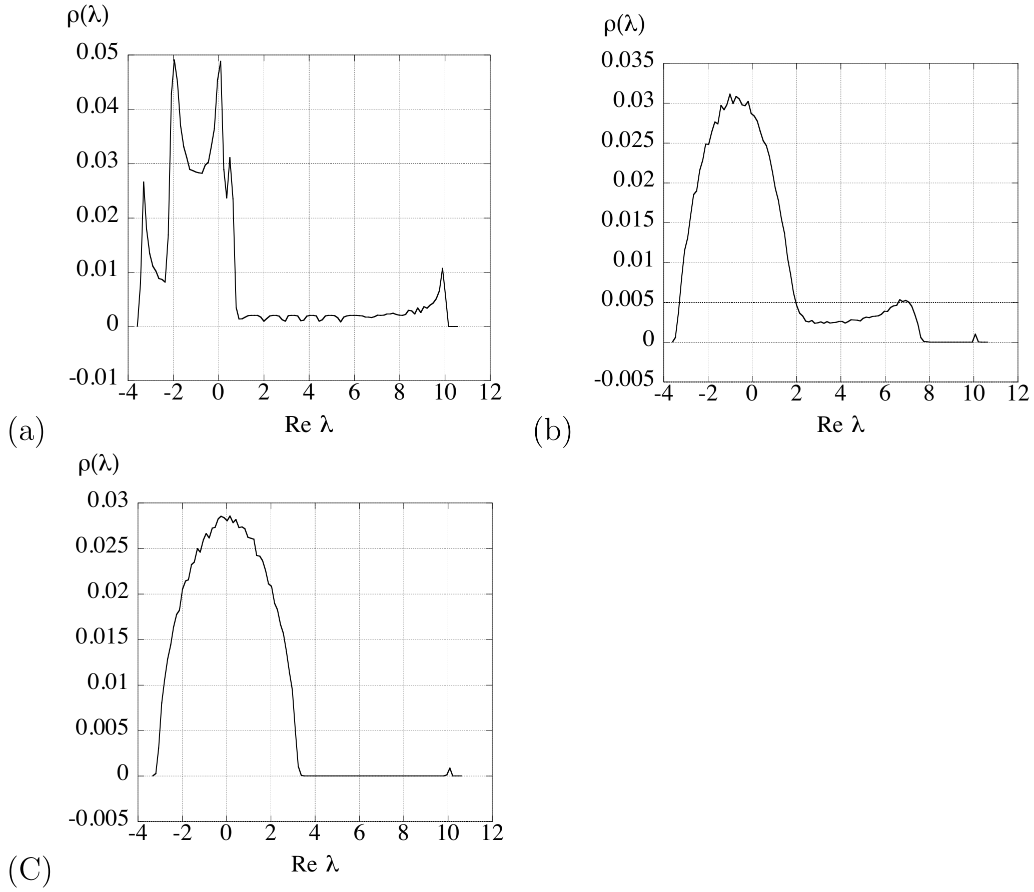

Figure 12: The density of the real part of the eigenvalues of the model C for (a) $p = 0.01$, (b) $p = 0.3$ and (c) $p = 1$. We used graphs with $N = 1000$ and $\langle k \rangle = 10$. In all three cases, we used one hundred graphs for averaging.

Thus, we arrive at the following conclusion: The ring structure of complex spectrum represents the existence of some kind of a directed loop with many steps, or the existence of a loop-like *flow* in the network.

(2) *Comparison with undirected spectra*: The real part and the imaginary part of the complex eigenvalues have information of its own. Here, we focus on the role of the real part of the eigenvalues and show that the real part reflects the undirected topology of the graph. Figure 12 shows the density of the *real part of the eigenvalues* of the directed Watts-Strogatz model starting from an undirected regular lattice ($p_1 = p_2 = 0$) and randomly replace edges with directed edges. Let us call this the model C.

Compare Fig. 12 with Fig. 8; we can see similarity between the spectral density of the undirected Watts-Strogatz model and the density of the real part of the eigenvalues of the model C.

We can explain this by perturbation. Let us write the adjacency matrix of the initial state in the following form

$$H_{\text{initial}} = 2\sum_{x=1}^{N}\sum_{n=1}^{k} |x\rangle\langle x+n|. \tag{14}$$

A periodic boundary condition is required for x. We perturb the system with two different kinds of noise.

Case 1: We randomly choose two nodes, a and b and add a new *undirected* link between them, which has the following form

$$\Delta H_{\text{undirected}} = |a\rangle\langle b| + |b\rangle\langle a|. \tag{15}$$

In this case, we obtain the first-order correction to the eigenvalues as follows:

$$\lambda_n^{(1)} = \frac{1}{N}\cos\frac{2\pi n}{N}(b-a). \tag{16}$$

Case 2: We add a *directed* link between the randomly chosen nodes:

$$\Delta H_{\text{directed}} = |a\rangle\langle b|. \tag{17}$$

In this case, we obtain the correction to the eigenvalues in the following form:

$$\lambda_n^{(1)} = \frac{1}{N}e^{\frac{2\pi n}{N}(b-a)} = \frac{1}{N}\big(\cos\frac{2\pi n}{N}(b-a) + i\sin\frac{2\pi n}{N}(b-a)\big). \tag{18}$$

We can see from Eqs. (16) and (18) that the correction due to the undirected noise (Eq. (15)) is the same as the real part of the correction due to the directed noise (Eq. (17)). This can be summarized as follows: if we ignore the directions of all edges of a directed graph, the spectral density of the resulting undirected graph is the same in the first-order approximation as the density of the real part of the eigenvalues of the directed graph. Thus, the distribution of the real part of the eigenvalues reflects the undirected topology of the graph and the imaginary part reflects the effect of directed links

(3) *Number of loops*: In undirected graphs, the graph spectrum is directly related to the number of loops in the network as shown in Eq. (7). Thus, we have the relation that the variance of the spectral density corresponds to the total number of edges in the network. In directed graphs, we can also relate the spectrum with the number of loops and obtain a similar relation: the variance of the distribution of the *imaginary part* of the eigenvalues approximately gives the number of *directed* edges.

Although it is more complicated than the undirected case, the number of directed loops may give us useful information. The number of loops with k steps, L_k, is given by calculating $L_k = \mathrm{Tr}(A^k)$, where A is the adjacency matrix of the network. In terms of the complex eigenvalues $\lambda_n = \alpha_n + i\beta_n$, the number of kth-order loops is given by

$$\begin{aligned} L_k &= \mathrm{Tr}(A^k) = \sum_{n=1}^{N} \lambda_n^k = \sum_{n=1}^{N} (\alpha_n + i\beta_n)^k \\ &= \sum_{n=1}^{N} \Big\{ \alpha_n^k + \sum_{m=1}^{<k/2} \binom{k}{m} \alpha_n^{k-2m} \beta_n^{2m} (-1)^n \Big\}. \end{aligned} \quad (19)$$

In the above calculations, we used the fact that the complex eigenvalues appear in a conjugate pair since A is a real matrix.

In directed networks, the number of loops with two steps L_2 is the number of bidirectional links:

$$L_2 = \sum_{n=1}^{N} (\alpha_n^2 - \beta_n^2). \quad (20)$$

Since $\langle \alpha \rangle = \langle \beta \rangle = 0$, we can rewrite Eq. (20) as

$$L_2 = N\sigma^2(\Re\lambda) - N\sigma^2(\Im\lambda), \quad (21)$$

where $\sigma^2(x)$ is the variance of the distribution of x. As we argued above, the distribution of the real part of the eigenvalues describes the undirected topology of the graph. Therefore, $N\sigma^2(\Re\lambda)$ approximately gives the total number of links in the network. Thus we can see that the variance of the imaginary part of the eigenvalues gives

$$\begin{aligned} N\sigma^2(\Im\lambda) &= N\sigma^2(\Re\lambda) - L_2 \\ &= \text{The number of the directed non-bidirectional edges.} \end{aligned} \quad (22)$$

5 Summary

We studied properties of directed networks, focusing on the *flow* in the network, which does not appear in undirected networks. First, we showed that directed small-world networks actually have a possibility of *flow*. We showed that one can obtain by spectral analysis, useful information on directed networks including the information on the *flow* in the complex network.

Acknowledgements

First, I would like to thank Prof. N. Hatano for a lot of help. I also acknowledge my friends, families and everybody who gave me the chance to write the thesis.

References

[1] P. Erdős and A. Rényi, "On random graphs," *Publicationes Mathematicae* **6** (1959) 290-297.

[2] D. J. Watts and S. H. Strogatz, "Collective dynamics of 'small-world' networks," *Nature* **393** (1998) 440-442.

[3] D. J. Watts, *Small Worlds: The Dynamics of Networks Between Order and Randomness (Princeton Reviews in Complexity)* (Princeton University Press, Princeton, New Jersey, 1999).

[4] A. Broder, R. Kumar, F. Maghoul, P. Raghavan, S. Rajagopalan, R. Stata, A. Tomkins and J. Wiener, "Graph structure in the web," *Comput. Netw.* **33**, 309.

[5] A. L. Barabási and R. Albert, "Emergence of scaling in random networks," *Science* **286** (1999) 509-512.

[6] M. E. J. Newman, "The structure of scientific collaboration networks: I. Network construction and fundamental results," *Phys. Rev. E* **64** (2001) 016131.

[7] M. E. J. Newman, "The structure of scientific collaboration networks: II. Shortest paths, weighted networks, and centrality," *Phys. Rev. E* **64** (2001) 016132.

[8] M. Faloutsos, P. Faloutsos and C. Faloutsos, "On Power-Law Relationships of the Internet Topology," ACM SIGCOMM '99; *Comput. Commun. Rev.* **29** (1999) 251-263.

[9] H. Ebel, L. I. Mielsch and S. Bornholdt, "Scale-free topology of e-mail networks," *Phys. Rev. E* **66** (2002) 035103(R).

[10] J. M. Montoya and R. V. Solé, "Small world patterns in food webs," cond-mat/0011195.

[11] A. Vazquez, "Statistics of citation networks," cond-mat/0105031.

[12] I. J. Farkas, I. Derényi, A. L. Barabási and T. Vicsek, "Spectra of 'real-world' graphs: Beyond the semicircle law," *Phys. Rev. E* **63** (2001) 026704.

[13] F. Juhász, "On the spectrum of random graph," *Colloq. Math. Soc. János Bolyai* (1978) 313-316.

[14] M. L. Mehta, *Random Matrices* (Academic, New York, 1991).